

Vibration Analysis of a Deploying and Spinning Beam with a Time-dependent Spinning Speed

시간에 따라 변하는 회전 속도와 함께 회전하며 전개하는 보의 진동 분석

Kefei Zhu* and Jintai Chung†
주극비·정진태

(Received November 5, 2015 ; Revised November 5, 2015 ; Accepted November 25, 2015)

Key Words : Deploying Beam(전개하는 보), Spinning Beam(회전하는 보), Time-dependent Spinning Speed(시간에 따라 변하는 회전 속도), Beat Phenomenon(맥놀이 현상)

ABSTRACT

This paper presents the vibration analysis of a deploying beam with spin when the beam has a time-dependent spinning speed. In the previous studies for the deploying beams with spin, the spinning speed was time-independent. However, it is more reasonable to consider the time-dependent spinning speed. The present study introduces the time-dependent spinning speed in the modeling. The Euler-Bernoulli beam theory and von Karman nonlinear strain theory are used together to derive the equations of motion. After the equations of motion are transformed into the weak forms, the weak forms are discretized. The natural frequency and dynamic response are obtained. The effect of the time-dependent spinning speed on the dynamic response is studied.

요 약

이 논문은 시간에 따라 변하는 회전 속도와 함께 전개하며 회전하는 보의 진동을 분석하였다. 전개하며 회전하는 보와 관련된 이전 연구들에서 회전 속도는 시간에 독립적이었다. 하지만, 시간에 따라 변하는 회전속도로 고려하는 것이 더 적합하다. 현재 연구는 모델링에서 시간에 따라 변하는 회전 속도를 소개하였다. 운동방정식을 유도하기 위해 오일러-베르누이(Euler-Bernoulli) 보 이론과 본 카르만(von Karman) 비선형 변형률 이론이 함께 사용되었다. 운동방정식을 약형(weak form)으로 변환한 후, 약형은 이산화 되었다. 고유 진동수와 시간응답을 얻었고, 시간에 따라 변화하는 회전 속도가 시간응답에 미치는 영향이 연구되었다.

1. Introduction

The vibration problems for the deploying beams and spinning beams are very important because

these beams are used in various mechanical systems, such as robot manipulators, deploying appendages on satellite, drilling machines in productions. Numerous reports have been published for the vibration analysis of these beams.

† Corresponding Author ; Member, Hanyang University
E-mail : jchung@hanyang.ac.kr
* Hanyang University

‡ Recommended by Editor Heung Soo Kim
© The Korean Society for Noise and Vibration Engineering

Some researchers analyzed the vibration of the deploying beams without a spinning motion. AI-Bedoor and Khuilief⁽¹⁾ derived an approximate analytical solution for the transverse vibrations of a beam during axial de-ployment. Park et al.⁽²⁾ analyzed the longitudinal and tra-nsvrse vibrations of an axially moving beam when the beam has deploying or retracting motion. The transverse vibration for the axially moving nested beam with a tip mass was studied by Duan et al.⁽³⁾. Kim and Chung⁽⁴⁾ presented a residual vibration reduction method for a flexible beam deployed from a translating hub.

Other papers were published for the spinning beams without deployment. Fung and Lee⁽⁵⁾ presented a para-metric variable structure control for the spinning beam. Young and Gau⁽⁶⁾ studied the dynamic stability of a beam spinning along its axial axis and subjected to an axial force. Sheu and Yang⁽⁷⁾ investigated the whirl speed, critical speed and mode shape of a spinning beam. A geometric nonlinear dynamic model for marine propulsion was established by Zou et al.⁽⁸⁾.

Although many papers have been published for the vibration analysis of the deploying beams without spin as well as the spinning beams without deployment, few papers have been published for the vibration of the beam with both deploying and spinning motion. Lee⁽⁹⁾ analyzed the vibration of a pre-twisted beam with deployment. Zhu and Chung⁽¹⁰⁾ studied the nonlinear vibration of a deploying beam with spin. In the above previous studies for the deploying beams with spin, the spinning speeds were time-independent. However, in practice, the spinning speed changes with time, it is more reasonable that the spinning speed is assumed to be time-dependent.

This study presents the vibration analysis of a deploying and spinning beam with a time-dependent spinning speed. The Euler-Bernoulli beam theory and the von Karman nonlinear strain theory are used together to derive the equation of

motion. The Galerkin method is used to discretize the equations. The natural frequency and dynamic response are obtained. The effect of the time-dependent spinning speed on the dynamic response is investigated.

2. Dynamic Modeling

Figure 1 shows the dynamic model of a spinning beam deploying from a rigid hub. The beam axially deploys with the time-dependent moving speed $V(t)$, and simultaneously spins along its axial axis with the time-dependent spinning speed $\Omega(t)$. The beam is uniform and it has mass density ρ , total length L , circular cross section with area A and area moment of inertia I . The length outside the hub is l . An external axial force F , which is applied at the left end, pushes the beam deploying out the hub.

The position vector can be defined by the axial displacement u , the lateral displacements v and w . The torsional displacement is not considered in this study because there is no coupling between torsional and lateral displacements for a spinning beam with the doubly symmetric cross section. The position vector of the point at a distance x away from the hub may be written as.

$$\mathbf{r} = \begin{cases} (x+u)\mathbf{i} & \text{for } l-L \leq x \leq 0 \\ (x+u)\mathbf{i} + v\mathbf{j} + w\mathbf{k} & \text{for } 0 \leq x \leq l \end{cases} \quad (1)$$

The Euler-Bernoulli beam theory and the von Karman nonlinear strain theory are used together to model the deploying beam with spin. It is assumed the beam is slender enough, so the rotary inertia and shear deformation can be neglected and the Euler-Bernoulli beam theory can be adopted. On the other hand, the von Karman nonlinear strain theory, which considers the geometric nonlinear due to the large deflection, is more adequate than the conventional linear strain theory.

The equations of motion can be derived by the

extended Hamilton's principle. By considering the time-dependent spinning speed and using the similar derivation procedure presented by the authors⁽¹⁰⁾, the equations of the axial and lateral motions may be derived and given as

$$\rho A \left(\frac{\partial^2 u}{\partial t^2} + 2V \frac{\partial^2 u}{\partial x \partial t} + V^2 \frac{\partial^2 u}{\partial x^2} + \dot{V} \frac{\partial u}{\partial x} \right) - EA \frac{\partial^2 u}{\partial x^2} = -\rho A \dot{V} \tag{1}$$

$$\rho A \left(\frac{\partial^2 v}{\partial t^2} + 2V \frac{\partial^2 v}{\partial x \partial t} + V^2 \frac{\partial^2 v}{\partial x^2} + \dot{V} \frac{\partial v}{\partial x} - \Omega^2 v \right) + EI \frac{\partial^4 v}{\partial x^4} - \rho A \left(2\Omega \frac{\partial w}{\partial t} + 2V\Omega \frac{\partial w}{\partial x} + \dot{\Omega} w \right) - EA \frac{\partial}{\partial x} \left(\frac{\partial u}{\partial x} \frac{\partial v}{\partial x} \right) = 0 \tag{2}$$

$$\rho A \left(\frac{\partial^2 w}{\partial t^2} + 2V \frac{\partial^2 w}{\partial x \partial t} + V^2 \frac{\partial^2 w}{\partial x^2} + \dot{V} \frac{\partial w}{\partial x} - \Omega^2 w \right) + EI \frac{\partial^4 w}{\partial x^4} + \rho A \left(2\Omega \frac{\partial v}{\partial t} + 2V\Omega \frac{\partial v}{\partial x} + \dot{\Omega} v \right) - EA \frac{\partial}{\partial x} \left(\frac{\partial u}{\partial x} \frac{\partial w}{\partial x} \right) = 0 \tag{3}$$

The associate boundary conditions are

$$EA \frac{\partial u}{\partial x} = -\rho A L \dot{V} \text{ at } x = l - L \tag{4}$$

$$EA \frac{\partial u}{\partial x} = 0 \text{ at } x = l \tag{5}$$

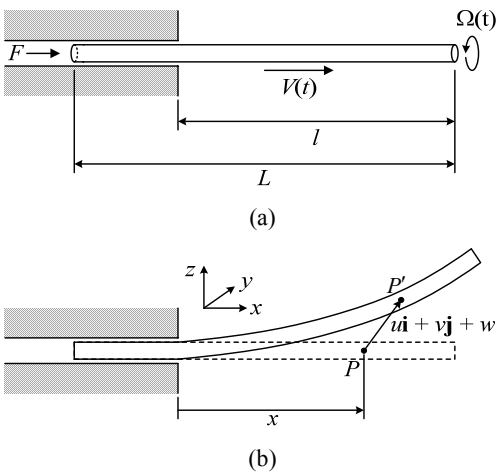


Fig. 1 Dynamic model of a deploying beam with spin

$$v = \frac{\partial v}{\partial x} = w = \frac{\partial w}{\partial x} = 0 \text{ at } x = 0 \tag{6}$$

$$EI \frac{\partial^2 v}{\partial x^2} = EI \frac{\partial^3 v}{\partial x^3} = EI \frac{\partial^2 w}{\partial x^2} = EI \frac{\partial^3 w}{\partial x^3} = 0 \text{ at } x = l \tag{7}$$

Note that in the lateral equations of motion, the spinning speed is the time function and it introduces the angular acceleration $\dot{\Omega}$ and two new corresponding terms $-\rho A \dot{\Omega} w$ and $\rho A \dot{\Omega} v$. These two terms bring about linear coupling effect on the lateral equations.

In order to derive the weak form, the trial functions and weighting functions are defined. The trial functions are defined by u, v and w , while the weighting functions are defined by \bar{u}, \bar{v} and \bar{w} . The weak forms, which may be derived by multiplying the equations of motion by weighting functions and integrating by parts over the domain, are given as

$$\rho A \int_{l-L}^l \bar{u} \left(\frac{\partial^2 u}{\partial t^2} + 2V \frac{\partial^2 u}{\partial x \partial t} + \dot{V} \frac{\partial u}{\partial x} \right) dx + (EA - \rho A V^2) \int_{l-L}^l \frac{\partial \bar{u}}{\partial x} \frac{\partial u}{\partial x} dx \tag{8}$$

$$= -\rho A \dot{V} \int_{l-L}^l \bar{u} dx + \left(1 - \frac{V^2}{E/\rho} \right) \rho A L \dot{V} \bar{u} \Big|_{x=l-L}$$

$$\int_0^l \rho A \bar{v} \left(\frac{\partial^2 v}{\partial t^2} + 2V \frac{\partial^2 v}{\partial x \partial t} + V^2 \frac{\partial^2 v}{\partial x^2} + \dot{V} \frac{\partial v}{\partial x} - \Omega^2 v \right) dx - \int_0^l \rho A \bar{v} \left(2\Omega \frac{\partial w}{\partial t} + 2V\Omega \frac{\partial w}{\partial x} + \dot{\Omega} w \right) dx + \int_0^l \left(EA \frac{\partial \bar{v}}{\partial x} \frac{\partial u}{\partial x} \frac{\partial v}{\partial x} + EI \frac{\partial^2 \bar{v}}{\partial x^2} \frac{\partial^2 v}{\partial x^2} \right) dx = 0 \tag{9}$$

$$\int_0^l \rho A \bar{w} \left(\frac{\partial^2 w}{\partial t^2} + 2V \frac{\partial^2 w}{\partial x \partial t} + V^2 \frac{\partial^2 w}{\partial x^2} + \dot{V} \frac{\partial w}{\partial x} - \Omega^2 w \right) dx + \int_0^l \rho A \bar{w} \left(2\Omega \frac{\partial v}{\partial t} + 2V\Omega \frac{\partial v}{\partial x} + \dot{\Omega} v \right) dx \tag{10}$$

$$+ \int_0^l \left(EA \frac{\partial \bar{w}}{\partial x} \frac{\partial u}{\partial x} \frac{\partial w}{\partial x} + EI \frac{\partial^2 \bar{w}}{\partial x^2} \frac{\partial^2 w}{\partial x^2} \right) dx = 0$$

The trial functions for the axial and lateral motions may be expressed as a series of the basis functions, which are given as

$$u(x, t) = \sum_{j=1}^N T_j^u(t) U_j(x, t) \tag{11}$$

$$v(x, t) = \sum_{n=1}^N T_n^v(t) V_n(x, t) \tag{12}$$

$$w(x, t) = \sum_{q=1}^N T_q^w(t) W_q(x, t) \tag{13}$$

Here N is number of the basis functions, the basis functions can be given as

$$U_j(x, t) = \sqrt{\frac{2}{L}} \cos \frac{j\pi}{L} [x - l(t) + L] \tag{14}$$

$$V_n = W_n = \frac{1}{\sqrt{l}} \left[\cosh \beta_n x - \cos \beta_n x - \frac{\sinh \beta_n l - \sin \beta_n l}{\cosh \beta_n l + \cos \beta_n l} (\sinh \beta_n x - \sin \beta_n x) \right] \tag{15}$$

where β_n is the n th solution of the frequency equation of $\cosh \beta_n l \cos \beta_n l + 1 = 0$.

The discretized equations are obtained by substituting the trial functions and weighting functions into the weak forms. The derived discretized equations may be written as in a matrix-vector form

$$\mathbf{M}_u \ddot{\mathbf{T}}_u + \mathbf{G}_u \dot{\mathbf{T}}_u + \mathbf{K}_u \mathbf{T}_u = \mathbf{F}_u \tag{16}$$

$$\begin{bmatrix} \mathbf{M}_v & \mathbf{0} \\ \mathbf{0} & \mathbf{M}_w \end{bmatrix} \begin{Bmatrix} \ddot{\mathbf{T}}_v \\ \ddot{\mathbf{T}}_w \end{Bmatrix} + \begin{bmatrix} \mathbf{G}_v & \mathbf{G}_{vw} \\ \mathbf{G}_{wv} & \mathbf{G}_w \end{bmatrix} \begin{Bmatrix} \dot{\mathbf{T}}_v \\ \dot{\mathbf{T}}_w \end{Bmatrix} + \begin{bmatrix} \mathbf{K}_v + \mathbf{K}_{vu} & \mathbf{K}_{vw} \\ \mathbf{K}_{wv} & \mathbf{K}_w + \mathbf{K}_{wu} \end{bmatrix} \begin{Bmatrix} \mathbf{T}_v \\ \mathbf{T}_w \end{Bmatrix} = \begin{Bmatrix} \mathbf{0} \\ \mathbf{0} \end{Bmatrix} \tag{17}$$

3. Analysis and Discussion

The dynamic responses and natural frequencies are obtained based on the above derived matrix

vector form. Before computation of the dynamic responses, the convergence tests should be performed. According to the results given by Zhu and Chung⁽¹⁰⁾, ten basis functions are reasonable for computations of the natural frequencies and dynamic responses.

The dynamic responses for the time-dependent moving speed and time-dependent spinning speed are computed. The material properties used for computation are beam diameter $d = 0.01$ m, total length $L = 10$ m, initial deployed length $l(0) = 2$ m, mass density 2738.6 kg/m³, Young's modulus $E = 6.8335 \times 10^{10}$ N/m², the initial deflection for the

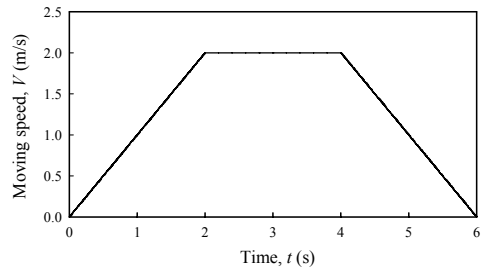
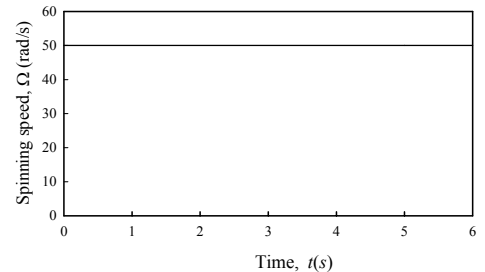
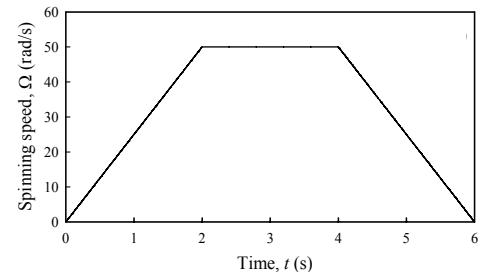


Fig. 2 Moving speed profile



(a) Constant case



(b) Time-dependent case

Fig. 3 The spinning speed profile

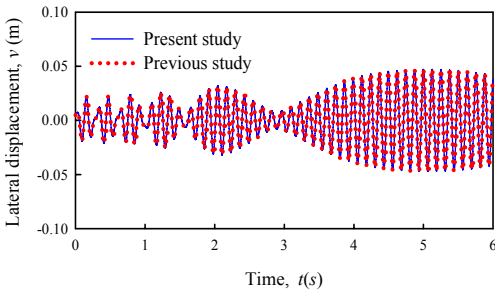
lateral displacement v is given as 5 mm. The time-dependent moving speed profile is given in Fig. 2, while the spinning speed profile is also given in Fig. 3. Two cases are considered for comparison. Fig. 3(a) is a constant case and Fig. 3(b) is a time-dependent case.

The dynamic response for the constant case is presented in Fig. 4. As shown in this figure, the dynamic response computed by this study is in agreement with that by the previous study⁽¹⁰⁾. It is observed the beat phenomenon occurs. According to the results given by the authors⁽¹⁰⁾, the beat phenomenon occurs due to interference of the first and second natural frequencies of the beam.

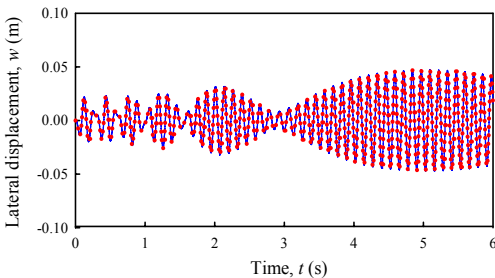
The effect of the time-dependent spinning speed on the dynamic response is investigated. Fig. 5 shows the dynamic response for the time-dependent spinning speed profile of Fig. 3(b). As shown in Fig. 5, at the initial stage, lateral v starts from 5 mm while w starts from 0 mm. This is because spin introduces gyroscopic effect. When one of

the lateral displacements is excited, the other one is also excited. Note that the magnitude of the lateral displacement in Fig. 5 is smaller than that in Fig. 4 because the initial spinning speed for the time-dependent case is smaller than the constant spinning speed.

At the accelerating interval from 0 s to 2 s, the period decreases with time. This phenomenon is because the spinning speed increases. At the constant speed interval from 2 s to 4 s, the beat phenomenon occurs. The beat phenomenon occurs due to the interference of the first and second natural frequencies of the spinning beam as mentioned before. At the decelerating interval from 4 s to 6 s, the period increases. This is because the beam length increases and spinning speed decreases. It is also found that compared with the previous studies, the beat phenomenon disappears at the decelerating interval. This difference between the present and previous studies may be caused by the effect of the time-dependent spinning speed.

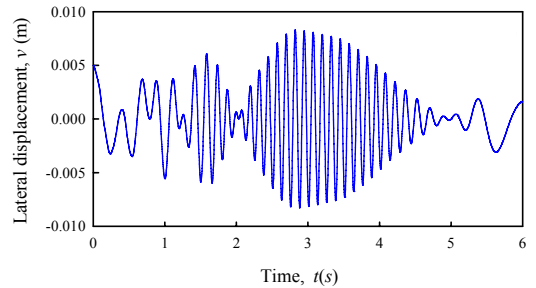


(a) Lateral v

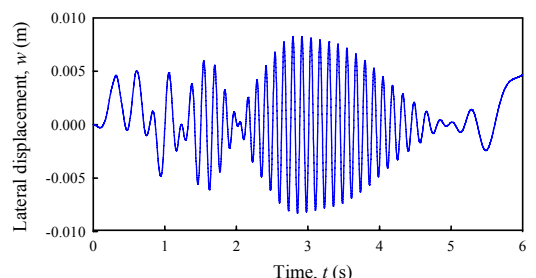


(b) Lateral w

Fig. 4 Verification of the lateral displacements for the constant spinning speed case



(a) Lateral v



(b) Lateral w

Fig. 5 Lateral displacements for the time-dependent spinning speed

It is necessary to investigate the disappearance of the beat phenomenon in the decelerating interval. According to the conclusion in the previous study, the beat phenomenon occurs due to the first and second natural frequencies of the spinning beam. The first and second natural frequencies are given as

$$\omega_1 = \left| 1.8751^2 \sqrt{EI/\rho AI^4} - \Omega \right| \tag{18}$$

$$\omega_2 = \left| 1.8751^2 \sqrt{EI/\rho AI^4} + \Omega \right| \tag{19}$$

The difference of the first and second natural frequencies ($\omega_2 - \omega_1$) is computed versus the combination of the spinning speed and beam length, and plotted in Fig. 6. As shown in this figure, when the beam length increases, the difference becomes smaller, and the beat phenomenon occurs. It should be noted that, for a certain beam length, the differences are similar whether the spinning speed is high or low. So the difference of the first and second natural frequencies may be not enough to explain and another new criterion needs to be proposed.

To explain the disappearance of the beat phenomenon in the decelerating interval, we investigate the difference ratio of the first and second natural frequencies versus the combination of the spinning speed and beam length. The difference ratio can be used to evaluate the relative difference and it may be written as

$$\Delta\omega = (\omega_2 - \omega_1) / \omega_1 \tag{20}$$

The difference ratio may be used to explain the disappearance of the beat phenomenon in the decelerating interval. The difference ratio versus the spinning speed and beam length are computed and plotted in Fig. 7. As shown in this figure, at the initial stage (region A), the spinning speed is low and the beam length is short, the difference ratio is large, beat does not occur. At the middle stage

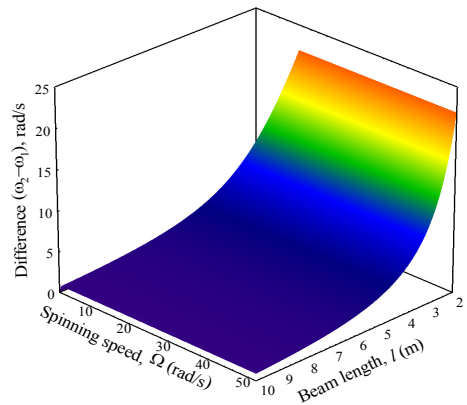


Fig. 6 Difference of first and second natural frequencies versus spinning speed and beam length

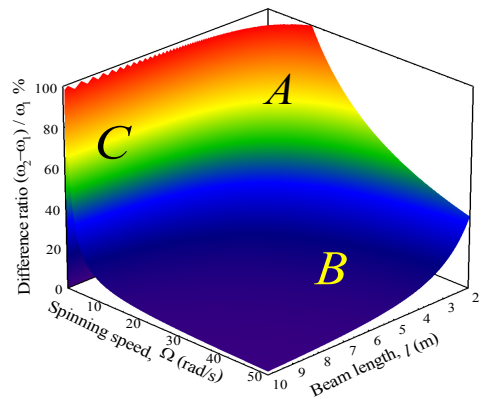


Fig. 7 Difference ratio of first and second natural frequencies versus spinning speed and beam length

(region B), the beam has a medium length and a high spinning speed, the difference ratio becomes small, the beat occurs. At the later stage (region C), the speed becomes low and the length becomes long, the difference ratio becomes large again, the beat phenomenon disappears. Therefore, beat does not occur when the spinning speed is low and the beam length is long.

3. Conclusion

In this study, the vibration of a deploying and spinning beam is analyzed when the spinning

speed is time-dependent. The Euler-Bernoulli beam and the von Karman nonlinear strain are used to model the deploying beam with spin. By considering the time-dependent spinning speed, the new equations of motion with angular acceleration are derived. The Galerkin method is adopted to discretize the equations of motion. The effects of the time-dependent spinning speed on the dynamic responses are investigated. The dynamic responses for the case of the constant speed and the time-dependent spinning speed are compared. It is found during deployment, when the spinning speed decreases, the beat phenomenon may disappear because the difference ratio of the first and second natural frequencies is large.

Acknowledgement

This work was supported by a grant from the National Research Foundation of Korea, funded by the Korean government(MEST)(No. 2011-0017408).

References

- (1) Al-Bedoor, B. O. and Khulief, Y. A., 1996, An Approximate Analytical Solution of Beam Vibrations during Axial Motion, *Journal of Sound and Vibration*, Vol. 192, No. 1, pp. 159~171.
- (2) Park, S. P., Yoo, H. H. and Chung, J., 2013, Vibrations of an Axially Moving Beam with Deployment or Retraction, *AIAA Journal*, Vol. 51, No. 3, pp. 686~696.
- (3) Duan, Y. C., Wang, J. P., Wang, J. Q., Liu, Y. W. and Shao, P., 2014, Theoretical and Experimental Study on the Transverse Vibration Properties of an Axially Moving Nested Cantilever Beam, *Journal of Sound and Vibration*, Vol. 333, No. 13, pp. 2885~2897.
- (4) Kim, B. and Chung, J., 2014, Residual Vibration Reduction of a Flexible Beam Deploying from a Translating Hub, *Journal of Sound and Vibration*, Vol. 333, No. 16, pp. 3759~3775.
- (5) Fung, R. F. and Lee, J. P., 1999, Parametric Variable Structure Control of a Spinning Beam System via Axial Force, *Journal of Sound and Vibration*, Vol. 227, No. 3, pp. 545~554.
- (6) Young, T. H. and Gau, C. Y., 2003, Dynamic Stability of Spinning Pretwisted Beams Subjected to Axial Random Forces, *Journal of Sound and Vibration*, Vol. 268, No. 1, pp. 149~165.
- (7) Sheu, G. J. and Yang, S. M., 2005, Dynamic Analysis of a Spinning Rayleigh Beam, *International Journal of Mechanical Sciences*, Vol. 47, No. 2, pp. 157~169.
- (8) Zou, D., Rao, Z. and Na, T., 2015, Coupled Longitudinal-transverse Dynamics of a Marine Propulsion Shafting under Superharmonic Resonances, *Journal of Sound and Vibration*, Vol. 346, No. 23, pp. 248~264.
- (9) Lee, H. P., 1994, Vibration of a Pretwisted Spinning and Axially Moving Beam, *Computers and Structures*, Vol. 52, No. 3, pp. 595~601.
- (10) Zhu, K. and Chung, J., 2015, Nonlinear Lateral Vibrations of a Deploying Euler-Bernoulli Beam with a Spinning Motion, *International Journal of Mechanical Sciences*, Vol. 90, pp. 200~212.



Kefei Zhu received his B.S. degree in mechanical engineering from Harbin Institute of Technology, China in 2010. Currently he is a Ph.D. candidate in the Department of Mechanical Engineering, Hanyang University, Korea. His research interests are vibration and dynamics.



Jintai Chung received his B.S. and M.S. degrees in mechanical engineering from Seoul National University, Seoul, Korea in 1984 and 1986, respectively, and a Ph.D. degree in mechanical engineering from the University of Michigan, Ann Arbor, USA in 1992. He is now a professor in the Department of Mechanical Engineering, Hanyang University, Korea. His research fields are structure dynamics, vibration and noise.